MLF Experimental Report	提出日 Date of Report May 7, 2011
課題番号 Project No. 2011B0053 実験課題名 Title of experiment Deformation structure and fatigue damage in Ti alloys by in-situ neutron diffraction during cyclic tensile test 実験責任者名 Name of principal investigator Satoshi MOROOKA 所属 Affiliation Yokohama National University	装置責任者 Name of responsible person Stefanus HARJO 装置名 Name of Instrument/（BL No.） Engineering Diffractometer (BL-19) 実施日 Date of Experiment February 11, 2011 – February 14, 2011

試料、実験方法、利用の結果得られた主なデータ、考察、結論等を、記述して下さい。（適宜、図表添付のこと）
Please report your samples, experimental method and results, discussion and conclusions. Please add figures and tables for better explanation.

1. 試料 Name of sample(s) and chemical formula, or compositions including physical form.

A Ti-Fe-O-(N) based alloy was used in this investigation. The Ti-Fe-O alloy, which is a near a-type titanium alloy, has been proposed for a new high-strength titanium alloy. The alloy derives its strength from solid solution hardening by interstitial elements such as oxygen and nitrogen. The supersaturation of iron leads to retention of b phase, which is effective to refine a matrix structure. The chemical compositions of an alloy used in this studied were 0.994Fe, 0.386O, 0.003N, 0.003C, 0.013Si, 0.014Ni, 0.002Sn, 0.006Al, 0.01Cr, 0.0005H in mass%. And the scattering length density is 5.4×10^{10} cm^{-2}. The Ti-Fe-O alloy were prepared by hot-rolling at 1123 K to plates with 30mm in thickness after annealing at 1023K for 3.6ks. And then, the Ti-Fe-O alloy was prepared by groove-rolling at 973K for 1h. After that, the specimen was prepared by aging at 1173K and 1223K for 3.6ks to obtain equal and needle-shape duplex grain structure and full needle-shaped grain structure, which were named as 900-HGR and 950-HGR alloy.

2. 実験方法及び結果（実験がうまくいかなかった場合、その理由を記述してください。）
Experimental method and results. If you failed to conduct experiment as planned, please describe reasons.

Experimental method: Cylindrical tensile specimens with 5mm in diameter and 4mm in gauge length were machined. The time-of-flight (TOF) *in-situ* neutron diffraction measurements were performed using TAKUMI at J-PARC. A tensile-compressive tester was made in such a way that the central position of a specimen does not move when a specimen is elongated. The geometrical arrangement for diffraction measurement in the axial and the transverse directions of the specimen is illustrated in **Figure 1**. The sampling volume for neutron diffraction is wide range at the parallel position of the tensile specimen, so that bulky averaged information is obtained. The TOF diffraction was acquired with a count time of about 10min for sufficient scattering intensity to analyze the diffraction-profiles. The uncertainties in elastic lattice strain and the change in dislocation density measurements represent the statistical uncertainty in the single peak fitting, based upon the estimated standard deviations of the peak positions.

2. 実験方法及び結果（つづき） Experimental method and results (continued)

Figure 2 is schematic illustration to explain the experimental condition. At room temperature, cyclic testing was performed using a tensile-compressive tester under tensile-tensile cyclic-loading conditions at constant maximum and minimum load amplitudes of 0MPa and about 600MPa. The stress ratio is about 0.01. The cyclic frequency was 0.1Hz. Fatigue data were collected at N=0, 10, 20, 30 ~ 300 cycles. The plastic stain was evaluated by strain gauge method.

Experimental result: Examples of diffraction profiles obtained for 900-HGR and 950-HGR alloys are presented in **Figure 3**. The *hk.l* peak intensities in the axial and transverse directions are different, indicating recrystallized texture and, the background in the transverse direction was not linear due to the incoherent scattering. As seen in the axial direction, {*10.1*} peak was split off two peaks. These peaks were α- titanium phase and oxygen concentrated α-titanium phase (Ti_xO). Table 1 shows change in intensity on the heat-treatment at 1173K and 1223K for 1hour. This indicates recrystallized texture generation.

Table 1 Change in crystal orientation on the heat-treatment.

Sample	10.0	00.2	10.1
As-HGR	72	0	30
900-HGR	39.8	35.6	114
950-HGR	22.4	207.9	386.5

Figure 4 shows the residual plastic strain as a function of the fatigue cycle using of strain gauge method. In case of 900-HGR, the residual plastic strain increases with increasing of the number of cycles. This means increasing of the dislocation density during cyclic deformation. However, in case of 950-HGR, in the beginning, the residual plastic strain rapid increases with increasing of the number of cycles. And then, the residual plastic strain decreases with increasing of the number of cycles. This means dislocations induced by martensitic transformation (form equal structure toward needle structure) must be rearranged and some are annihilated during cyclic deformation.

Figure 5 shows the elastic lattice strain determined from peak shifts of {*10.0*}, {*00.2*} and {*10.1*} reflection peaks $\varepsilon_{10.0}$, $\varepsilon_{00.2}$ and $\varepsilon_{10.1}$, as a function of the number of cyclic deformation for 900-HGR (a) and 950-HGR (b) alloys. As is observed in (a), $\varepsilon_{10.0}$, $\varepsilon_{00.2}$ and $\varepsilon_{10.1}$ in the axial direction increase linearly till approximately 50 cycles. After 50 cycles, {*10.0*} and {*00.2*} elastic lattice strain increases slightly or not changes while {*10.1*} decreases with increasing of the number of cycles. This implies that the {*10.1*} family grains are plastically softer than {*10.0*} and {*00.2*} grains, resulting in stress partitioning that is called intergranular stresses. As is observed in (b), change in elastic lattice strain of 950-HGR much smaller than that of 900-HGR. This indicates that 950-HGR alloy is occurred the plastic strain relaxation. Needless to say, this means dislocations induced by martensitic transformation must be rearranged and some are annihilated during cyclic deformation.

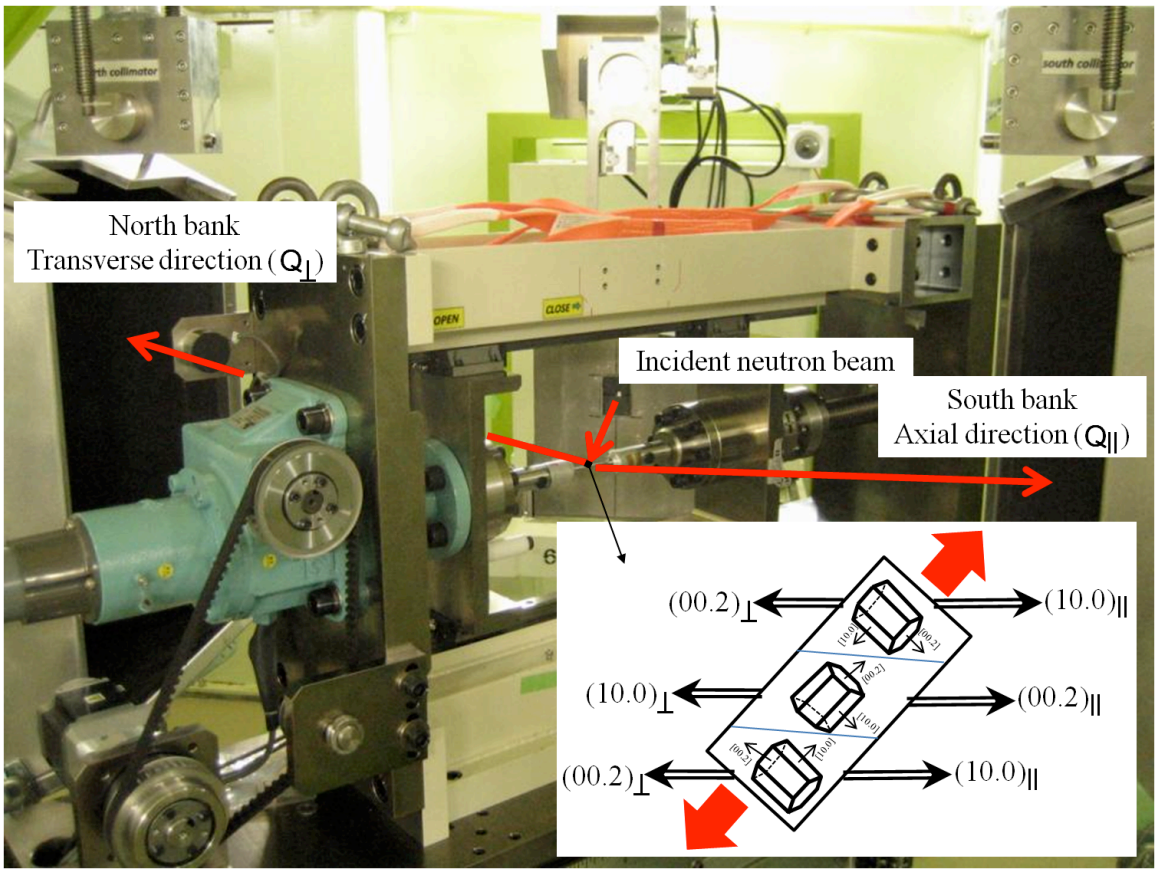

Figure 1 Schematic illustration of the diffraction geometry adopted on TAKUMI and the principle of collecting the *in-situ* neutron diffraction.

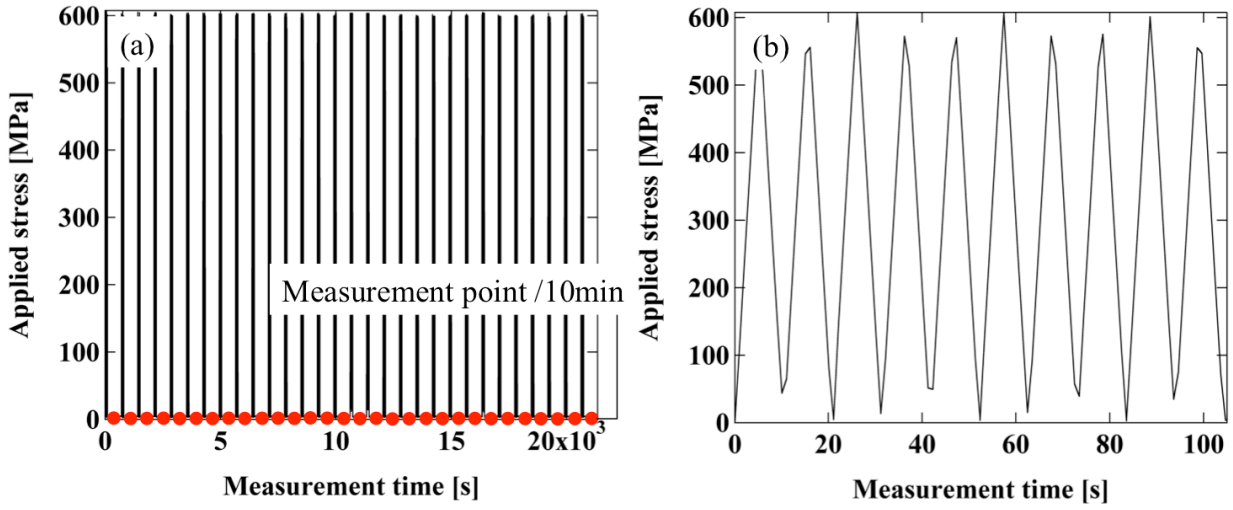

Figure 2 (a) The experimental schedules and (b) tensile-tensile cyclic loading condition.

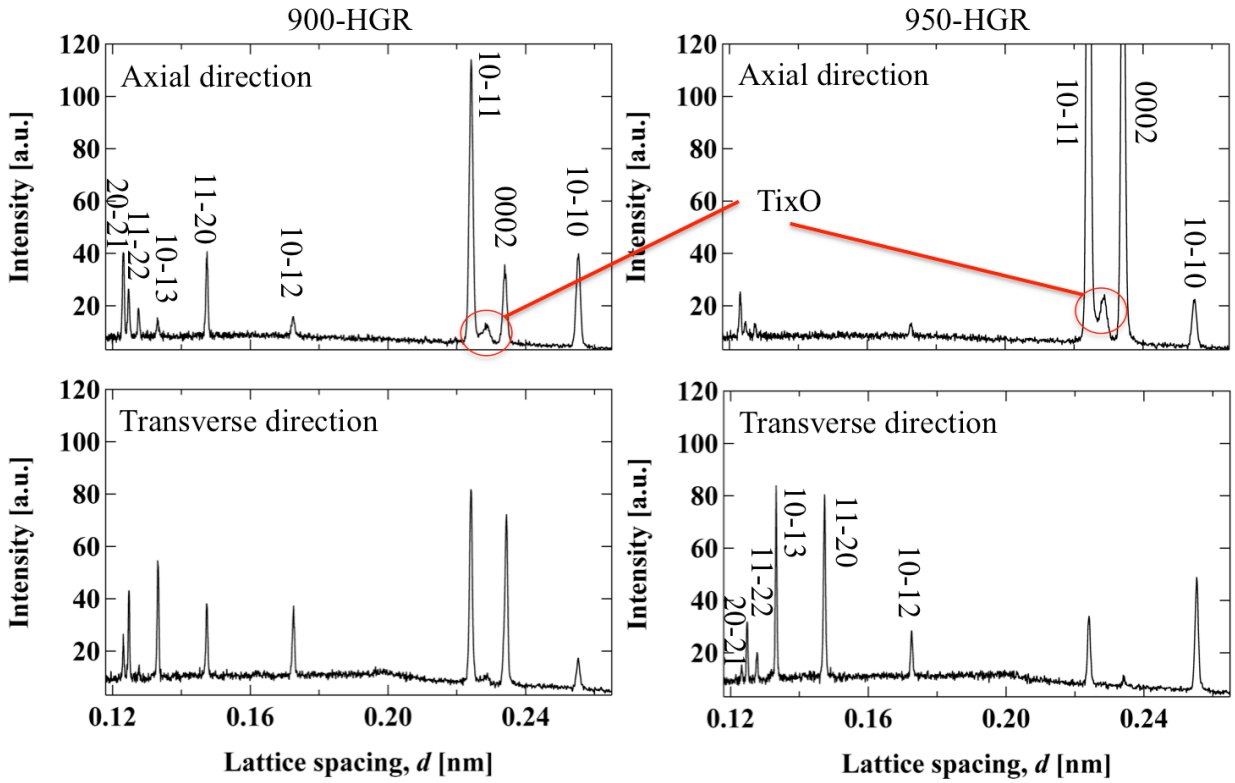

Figure 3 Diffraction profiles obtained during cyclic loading in the both directions for 900-HGR and 950-HGR alloys.

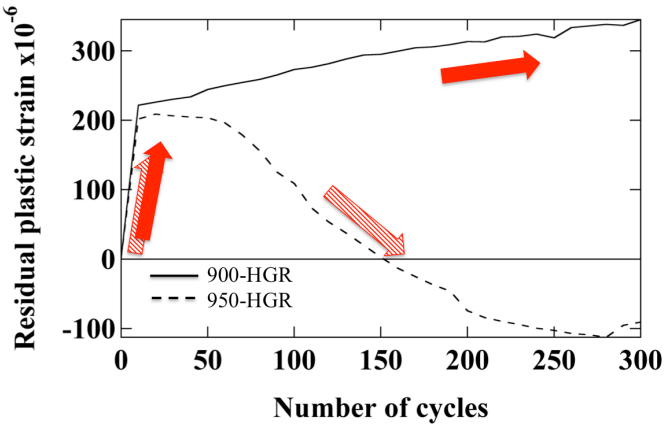

Figure 4 The residual plastic strain as a function of the number of cyclic deformation using of strain gauge method for 900-HGR and 950-HGR alloys. In case of 900-HGR, the residual plastic strain increases with increasing of fatigue cycles. However, in case of 950-HGR, in the beginning, the residual plastic strain rapid increases with increasing of fatigue cycles. And then, the residual plastic strain decreases with increasing of fatigue cycles.

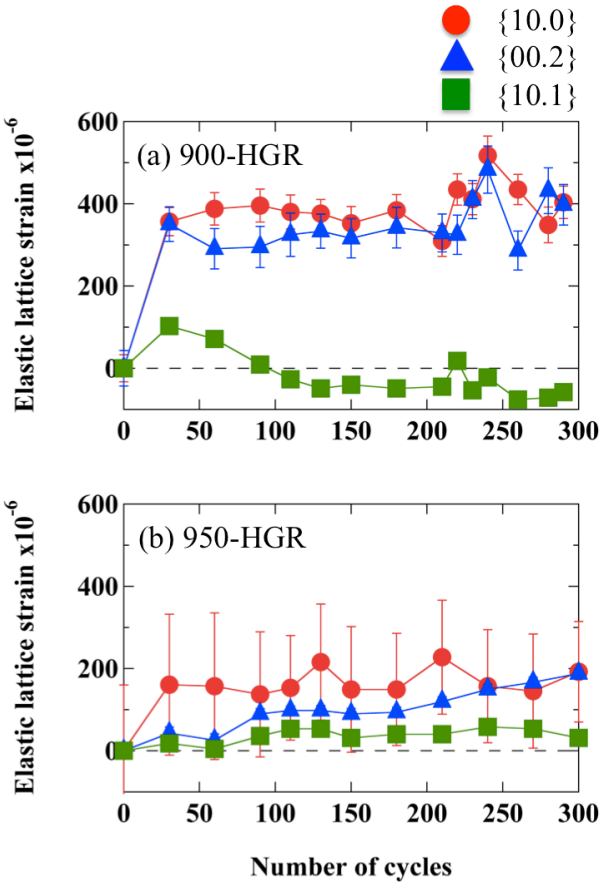

Figure 5 shows the elastic lattice strain determined from peak shifts of {10.0}, {00.2} and {10.1} reflection peaks $\varepsilon_{10.0}$, $\varepsilon_{00.2}$ and $\varepsilon_{10.1}$, as a function of the number of cyclic deformation for 900-HGR (a) and 950-HGR (b) alloys in the axial direction. The stress partitioning of 900-HGR is larger than that of 950-HGR.